EST기반 변조에서 8 PSK와 16 QAM에 대한 신호 검출

준회원 권 병 욱*, 종신회원 황 태 원*°

Signal Detection for 8 PSK and 16 QAM in EST-Based Modulation

Byung-uk Kwon* *Associate Member*, Teawon Hwang*° *Lifelong Member*

요 약

EST (Energy Spreading Transform) 기반의 변조는 광대역 무선통신에서 주파수 선택적 fading을 방지하는 효과적인 기술이다. 이 기법은 linear decoder의 복잡도를 가지면서 ISI (Inter-Symbol Interference)-free MFB (Matched Filter Bound)에 근접한 성능을 나타낸다. EST 기반의 변조는 원래 QPSK에 대해 제안되었다. 하지만, 다중 fading 채널의 capacity를 최대한 이용하기 위해서 higher-order의 변조방식이 필요하다. 본 논문에서는 QPSK에 대해 제안되었던 기존 EST 기반 변조를 재검토하고, 이를 8 PSK와 16 QAM으로 확장하는 것을 논의한다. 확장한 시스템의 성능은 Proakis B 채널과 8-tap fading 채널에서의 가상실험을 통해 검증되었다. 8 PSK로 확장한 EST기반의 시스템은 MFB에 매우 근접한 성능을 보여주었지만 16 QAM으로 확장한 EST기반의 시스템은 MFB와의 성능 차이를 보여주었다.

Key Words : EST, 다치 변조, 반복적 등화 방법, modulation

ABSTRACT

Energy spreading transform (EST) based modulation is an effective technique to combat frequency-selective fading in broadband wireless communication. It performs close to the inter-symbol interference (ISI)-free matched filter bound (MFB) only at the complexity of a linear detector. Originally, EST-based modulation has been proposed for QPSK. However, to fully utilize the capacity of multipath fading channels, higher-order modulations are also necessary. In this paper, we review the EST based modulation that has originally been proposed for QPSK and discuss its extension to 8 PSK and 16 QAM. The performance of the extended system is verified through simulation in Proakis B and 8-tap fading channel. The EST based modulation for 8 PSK shows the performance which is very close to MFB and the EST based modulation for 16 QAM shows the performance gap between its receiver and MFB.

I. Introduction

Energy spreading transform (EST) based modulation[1] is a powerful scheme to combat frequency selectivity of wireless channels for wideband communications. Like OFDM[2-5] and SC-FDE[6], EST-based modulation is a block-transmission scheme that employs cyclic prefix (CP) to prevent inter-block interference. Also, similar to SC-FDE, it employs low-complexity frequency-domain equalization to combat inter-symbol interference (ISI) in single-carrier broadband

※ 이 논문은 2010년도 정부(교육과학기술부)의 재원으로 한국연구재단의 지원을 받아 수행된 기초연구사업임. (No. 2011-0003277)
* 연세대학교 전기전자공학부 무선통신(WCL)연구실(ahlpa207@gmail.com, twhwang@yonsei.ac.kr), (° : 교신저자)
논문번호: KICS2011-03-164, 접수일자 : 2011년 3월 31일, 최종논문접수일자 : 2011년 11월 1일

communications.

EST spreads the symbol energy to the entire symbol block, increase the reliability of the feedback signal, and enables iterative signal detection at the receiver even without channel coding. Both hard-decision and soft-decision receivers have been developed for the iterative signal detection. At sufficiently high signal-to-noise ratio (SNR), it removes most of the ISI and its performance approaches the matched filter bound (MFB). However, its complexity is only that of a linear detector.

Originally, EST-based modulation has been proposed for QPSK[1]. However, to fully utilize the capacity of wireless multipath fading channels, higher-order modulations that can convey more bits per symbol than QPSK are also necessary. For example, in adaptive modulation, constellation size or modulation type is adapted to the channel condition to maximize the spectral efficiency[7-9]. To adapt to the wide range of channel SNR variation, modulation types such as BPSK, QPSK, 8 PSK, 16 QAM, 16 PSK, 32 PSK, 64 QAM, and 256 QAM are used.

In this paper, we consider the extension of EST-based modulation to higher order modulations. Optimum forward and feedback filters for 8 PSK and 16 QAM are derived for both hard and soft-decision receivers. Signal detections for higher-order PSK's and higher-order QAM's can be derived following our approaches used in the derivation of 8 PSK and 16 QAM, respectively.

The rest of the paper is organized as follows. System model for EST-based modulation is in Section II. Optimum receivers for both 8 PSK and 16 QAM with hard-decision and soft-decision schemes are provided in Section III and Section IV, respectively. Simulation results are provided in Section V and finally conclusion is drawn in Section VI.

Throughout this paper, *, ^{T}, and ^{H} denote complex conjugate, transpose, and Hermitian, respectively. $\odot$ denotes circular convolution and $\mathcal{E}\{\ \}$ denotes statistical expectation.

Ⅱ. System Model

Fig. 1 shows the block diagram of EST based modulation and its detection. A block of transmit symbols $\boldsymbol{s}=[s_0, s_1, \cdots, s_{N-1}]^T$ of length N with an average transmit power σ_s^2 is transformed by EST to

$$\tilde{\boldsymbol{s}}=[\tilde{s}_0, \tilde{s}_1, \cdots, \tilde{s}_{N-1}]^T=\boldsymbol{E}\boldsymbol{s}$$

where $\boldsymbol{E}$ is an N by N EST matrix. An EST is an orthonormal transform that uniformly spreads a symbol energy over the entire symbol block. Before transmission, a cyclic prefix (CP) is inserted to avoid interblock interference. At the receiver, CP is first extracted and then the received signal can be written as

$$r_n = h_n \odot \tilde{s}_n + n_n \tag{1}$$

where n_n denotes additive white Gaussian noise (AWGN) with power σ_n^2. Equivalently, (1) can be written in frequency domain as

$$R_k = H_k \tilde{S}_k + N_k$$

where R_k, H_k, and N_k are discrete Fourier transforms of r_n, h_n, and n_n, respectively.

The signal is detected in an iterative fashion by forward and feedback filters. Optimum forward filter depends on the reliability of feedback signal. Define

$$d_n^{(i)} \triangleq s_n - \hat{s}_n^{(i)}$$

to be the post-detection error, where $\hat{s}_n^{(i)}$ is the soft-

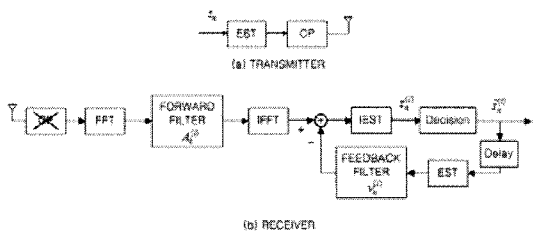

Fig. 1. EST-based modulation

or hard-decision of s_n at the ith iteration. As derived in [1], optimum forward filter in frequency-domain that maximizes signal to interference noise ratio (SINR) at the ith iteration is

$$A_k^{(i)} = \frac{\alpha H_K^*}{\left(\sigma_d^{(i-1)}\right)^2 |H_k|^2 + \sigma_n^2} \tag{2}$$

where α is a scaling factor and

$$\left(\sigma_d^{(i)}\right)^2 = \frac{1}{N}\sum_{n=0}^{N-1} \mathcal{E}\left\{|d_n^{(i)}|^2\right\} \tag{3}$$

is post-detection error power[1]. At the first iteration, $\left(\sigma_d^{(0)}\right)^2 = \sigma_s^2$ because there is no feedback signal. The feedback filter in time domain cancels the residual ISI after forward filtering[1], that is,

$$v_n^{(i)} \triangleq g_n^{(i)} - g_0^{(i)}\delta_n$$

where

$$g_n^{(i)} \triangleq \frac{1}{N}\sum_{k=0}^{N-1} A_k^{(i)} H_k e^{\frac{2\pi kn}{N}}$$

Then, consider the decision variable at the ith iteration right before the decision device in Fig. 1,

$$z_n^{(i)} = s_n + i_n^{(i)} + n'^{(i)}_n \tag{4}$$

where $i_n^{(i)}$ and $n'^{(i)}_n$ are interference and noise, respectively. Note that the coefficient of s_n is one by adequately choosing α in (2). Then, the signal, interference and noise power can be expresses as [1],

$$P_{\text{si}}^{(i)} = \sigma_s^2$$
$$P_{\text{in}}^{(i)} = K_h^{(i)}\left(\sigma_d^{(i-1)}\right)^2$$

and

$$P_{\text{no}}^{(i)} = \frac{\sigma_n^2}{N}\sum_{k=1}^{N-1}|A_k^{(i)}|^2$$

respectively, where

$$K_h^{(i)} \triangleq \frac{1}{\left(g_0^{(i)}\right)^2}\sum_{n\neq 0}|g_n^{(i)}|^2.$$

The SINR at the ith iteration is

$$\gamma^{(i)} = \frac{\sigma_s^2}{\left(\sigma_e^{(i)}\right)^2}$$

where $\left(\sigma_e^{(i)}\right)^2 = P_{\text{in}}^{(i)} + P_{\text{no}}^{(i)}$ is the error power at the ith iteration. For our analysis, we assume the interference plus noise to be Gaussian. Each variable in (4) can be decomposed into its real (in-phase) and imaginary (quadrature) components. For example, $z_n^{(i)} = z_{I,n}^{(i)} + jz_{Q,n}^{(i)}$ and $s_n = s_{I,n} + js_{Q,n}$. Also, the error power can be decomposed into

$$\left(\sigma_e^{(i)}\right)^2 = \left(\sigma_{e,I}^{(i)}\right)^2 + \left(\sigma_{e,Q}^{(i)}\right)^2.$$

Our objective is develop hard- and soft-detection schemes for 8 PSK and 16 QAM. The examples of the Gray mapping for M-ary constellation are shown in Table 1. For 8 PSK, a_l denotes the lth symbol in the constellation $A = \{a_l\}_{l=0}^{7}$. For 16 QAM, $a_{I,l}$ and $a_{Q,l}$ denote the lth symbol of a inphase and quadrature component in the constellation $A = \{a_{I,l} + j \cdot a_{Q,l}\}_{l=0}^{15}$, respectively. In the following sections, we calculate post-detection error

Table 1. Gray mapping for 8 PSK and 16 QAM.

8 PSK

l	α_l	$b_l^0 b_l^1 b_l^2$
0	1	000
1	$\frac{1}{\sqrt{2}}(1+j)$	001
2	j	011
3	$\frac{1}{\sqrt{2}}(-1+j)$	010
4	-1	110
5	$-\frac{1}{\sqrt{2}}(1+j)$	111
6	$-j$	101
7	$\frac{1}{\sqrt{2}}(1-j)$	100

16 QAM ($\alpha_l = \alpha_{I,l} + \alpha_{Q,l}$)

l	$\alpha_{I,l}(\alpha_{Q,l})$	$b_l^0 b_l^1 (b_l^2 b_l^3)$
0	-3	000
1	-1	001
2	1	011
3	3	010

power in (3) to be used in forward filter for 8 PSK and 16 QAM. For soft-decision scheme, we derive expressions for extrinsic log-likelihood ratio (LLR) and represent the soft decision in terms of the extrinsic LLR.

Ⅲ. Hard Decision

In this section, we describe the detection schemes for hard decisions. As shown in [1], (3) becomes

$$\left(\sigma_d^{(i)}\right)^2 = \mathcal{E}\left\{\left|d_n^{(i)}\right|^2 \middle| d_n^{(i)} \neq 0\right\} \cdot p^{(i)} \tag{5}$$

where $p^{(i)}$ is the symbol error rate (SER) for the ith iteration. As derived in Appendix A, the post-detection error power for 8 PSK and 16 QAM are

$$\begin{aligned}\left(\sigma_d^{(i)}\right)^2_{8\,\mathrm{PSK}} &\approx 1.172\,Q\left(\sqrt{0.293\gamma^{(i)}}\right)+4Q\left(\sqrt{\gamma^{(i)}}\right)\\ &\quad +6.828\,Q\left(\sqrt{1.707\gamma^{(i)}}\right)+4Q\left(\sqrt{2\gamma^{(i)}}\right)\end{aligned} \tag{6}$$

and

$$\begin{aligned}\left(\sigma_d^{(i)}\right)^2_{16\,\mathrm{QAM}} &\approx 12Q\left(\sqrt{\frac{\gamma^{(i)}}{5}}\right)+25.5Q\left(3\sqrt{\frac{\gamma^{(i)}}{5}}\right)\\ &\quad +25Q\left(5\sqrt{\frac{\gamma^{(i)}}{5}}\right)\end{aligned} \tag{7}$$

respectively.

Ⅳ. Soft Decision

In this section, we describe the detection schemes for soft decision. First, *a posteriori* LLR is defined in terms of *a priori* and *extrinsic* LLR. Then, the expressions for *extrinsic* LLR, soft decision, and post-detection error powers are derived in subsections 4.1, 4.2, and 4.3, respectively.

For each symbol $a_l \in A$ in Table 1, the corresponding bits are b_l^r for $r=0,\cdots,q$ where $q \triangleq \log_2 M - 1$. Denote

$$P_p^{(i)}(a_l) \triangleq P_p^{(i)}(s_n = a_l)$$

and

$$P_p^{(i)}(b_l^r) \triangleq P_p^{(i)}(x_n^r = b_l^r)$$

to be *a posteriori* probabilities of $s_n = a_l$ and $x_n^r = b_l^r$, respectively, where x_n^r denotes the rth bit of the nth symbol s_n. Note that l in a_l and b_l^r is the symbol index in A, while n in s_n and x_n^r is the time index. As shown in [10], assuming independence of x_n^r's, we have

$$P_p^{(i)}(a_l) = \prod_{r=0,\cdots,q} P_p^{(i)}(b_l^r)$$

where each b_l^r takes a value in $\{0,1\}$ depending on the considered symbol a_l.

The *a posteriori* LLR of x_n^r is defined by

$$L_p^{(i)}[x_n^r] \triangleq \ln\left[\frac{P_p^{(i)}(x_n^r=1)}{P_p^{(i)}(x_n^r=0)}\right]$$

for $r=0,\cdots,q$. It can be decomposed as

$$L_p^{(i)}[x_n^r] = L_e^{(i)}[x_n^r] + L_a^{(i)}[x_n^r],$$

where $L_e^{(i)}[x_n^r]$ and $L_a^{(i)}[x_n^r]$ are *extrinsic* LLR and *a priori* LLR of x_n^r at the ith iteration, respectively. As shown in [1], the *a priori* LLR is from the *extrinsic* LLR from the previous iteration, that is,

$$L_a^{(i)}[x_n^r] \triangleq \ln\left[\frac{P_a^{(i)}(x_n^r=1)}{P_a^{(i)}(x_n^r=0)}\right] \tag{8}$$

$$= L_e^{(i-1)}[x_n^r] \tag{9}$$

where $P_a(x_n^r=\omega)$ for $\omega \in \{0,1\}$ is *a priori* probability of $x_n^r=\omega$ at the ith iteration. Note that at the first iteration, $L_a^{(1)}[x_n^r]=0$ because no

a priori LLR is available.

4.1 Extrinsic LLR

Denote $P_e(x_n^r=\omega)$ to be *extrinsic* probability of $x_n^r=\omega$ at the ith iteration, then *extrinsic* LLR of x_n^r derived in [11] is

$$L_e^{(i)}[x_n^r] \triangleq \ln\left[\frac{P_e^{(i)}(x_n^r=1)}{P_e^{(i)}(x_n^r=0)}\right] \approx \ln\frac{\sum_{a_l:b_l^r=1} p(z_n^{(i)}|a_l)\left[\prod_{\substack{m=0,\cdots,q\\ m\neq r}} P_a^{(i)}(b_l^m)\right]}{\sum_{a_l:b_l^r=0} p(z_n^{(i)}|a_l)\left[\prod_{\substack{m=0,\cdots,q\\ m\neq r}} P_a^{(i)}(b_l^m)\right]} \quad (10)$$

where $a_l.b_l^r=\omega$ denotes the set of a_l's in A for which $b_l^r=\omega$,

$$p(z_n^{(i)}|a_l)=\exp\left[-\frac{|z_n^{(i)}-a_l|^2}{(\sigma_e^{(i)})^2}\right]$$

and

$$P_a^{(i)}(b_l^m) \triangleq P_a^{(i)}(x_n^m=b_l^m). \quad (11)$$

The *a priori* probability in (11) can be also represented as

$$P_a(b_l^m)=\begin{cases}\dfrac{1}{1+\exp(L_a^{(i)}[x_n^m])}, & (b_l^m=0)\\ \dfrac{\exp(L_a^{(i)}[x_n^m])}{1+\exp(L_a^{(i)}[x_n^m])}, & (b_l^m=1)\end{cases}. \quad (12)$$

For our further derivation of (10), define

$$\widehat{\max}(x,y) \triangleq \max(x,y)+\ln[1+\exp(-|x-y|)] \quad (13)$$

and

$$\widehat{\max}(x_1,x_2,x_3) \triangleq \widehat{\max}(\widehat{\max}(x_1,x_2),x_3) \quad (14)$$

For 8 PSK, as derived in Appendix B.1, the *extrinsic* LLR of the first bit $(r=0)$ is

$$\begin{aligned}L_e^{(i)}[x_n^0] &= \widehat{\max}(L_a^{(i)}[x_n^1]-f_1, L_a^{(i)}[x_n^1]+L_a^{(i)}[x_n^2]-f_3,\\ &\quad L_a^{(i)}[x_n^2]-f_2, f_4)-\widehat{\max}(f_1, L_a^{(i)}[x_n^2]+f_3,\\ &\quad L_a^{(i)}[x_n^1]+L_a^{(i)}[x_n^2]+f_2, L_a^{(i)}[x_n^1]-f_4)\end{aligned} \quad (15)$$

where

$$f_1 \triangleq 2z_{I,n}^{(i)}/(\sigma_e^{(i)})^2$$
$$f_2 \triangleq 2z_{Q,n}^{(i)}/(\sigma_e^{(i)})^2$$
$$f_3 \triangleq \sqrt{2}(z_{I,n}^{(i)}+z_{Q,n}^{(i)})/(\sigma_e^{(i)})^2$$

and

$$f_3 \triangleq \sqrt{2}(z_{I,n}^{(i)}-z_{Q,n}^{(i)})/(\sigma_e^{(i)})^2.$$

The *extrinsic* LLR's for the other bits $(r=1,2)$ can be similarly derived to be

$$\begin{aligned}L_e^{(i)}[x_n^1] &= \widehat{\max}(L_a^{(i)}[x_n^2]+f_2-f_4, L_a^{(i)}[x_n^0]-f_1,\\ &\quad L_a^{(i)}[x_n^0]+L_a^{(i)}[x_n^2]-f_3)-\widehat{\max}(f_1,\\ &\quad L_a^{(i)}[x_n^2]+f_3, L_a^{(i)}[x_n^0]+L_a^{(i)}[x_n^2]-f_2,\\ &\quad L_a^{(i)}[x_n^0]+f_4)\end{aligned} \quad (16)$$

and

$$\begin{aligned}L_e^{(i)}[x_n^2] &= \widehat{\max}(f_3, L_a^{(i)}[x_n^1]+f_2,\\ &\quad L_a^{(i)}[x_n^0]+L_a^{(i)}[x_n^1]-f_3, L_a^{(i)}[x_n^0]-f_2)\\ &\quad -\widehat{\max}(f_1, L_a^{(i)}[x_n^1]-f_4\\ &\quad L_a^{(i)}[x_n^0]+L_a^{(i)}[x_n^1]-f_1, L_a^{(i)}[x_n^0]+f_4)\end{aligned} \quad (17)$$

respectively.

For 16 QAM, as shown in Table 1, bits b_l^0,b_l^1 corresponds to $a_{I,l}$ while b_l^2,b_l^3 corresponds to $a_{Q,l}$. Using the similar method used for 8 PSK, the *extrinsic* LLR for x_n^0 and x_n^1 can be found to be

$$\begin{aligned}L_e^{(i)}[x_n^0] &= \widehat{\max}\left[L_a^{(i)}[x_n^1]+\frac{2z_{I,n}^{(i)}-1}{2(\sigma_{e,I}^{(i)})^2}, \frac{6z_{I,n}^{(i)}-9}{2(\sigma_{e,I}^{(i)})^2}\right]\\ &\quad -\widehat{\max}\left[\frac{-6z_{I,n}^{(i)}-9}{2(\sigma_{e,I}^{(i)})^2}, L_a^{(i)}[x_n^1]-\frac{2z_{I,n}^{(i)}+1}{2(\sigma_{e,I}^{(i)})^2}\right]\end{aligned} \quad (18)$$

and

$$L_e^{(i)}[x_n^1] = \widehat{\max}\left[\frac{-2z_{I,n}^{(i)}-1}{2(\sigma_{e,I}^{(i)})^2}, L_a^{(i)}[x_n^1] + \frac{2z_{I,n}^{(i)}-1}{2(\sigma_{e,I}^{(i)})^2},\right] - \widehat{\max}\left[\frac{-6z_{I,n}^{(i)}-9}{2(\sigma_{e,I}^{(i)})^2}, L_a^{(i)}[x_n^1] + \frac{6z_{I,n}^{(i)}-9}{2(\sigma_{e,I}^{(i)})^2}\right] \quad (19)$$

where (18) is proved in Appendix B.2 and (19) can be similarly derived. The remaining bit LLR's $L_e^{(i)}[x_n^2]$ and $L_e^{(i)}[x_n^3]$ can be similarly expressed in terms of $(\sigma_{e,Q}^{(i)})^2$ and $z_{Q,n}^{(i)}$.

4.2 Soft Decision

The soft decision of $s_n^{(i)}$ which is input to the feedback filter at the $(i+1)$th iteration is

$$\hat{s}_n^{(i)} \triangleq \sum_{l=0}^{M-1} a_l P_a^{(i+1)}(a_l) = \hat{s}_{I,n}^{(i)} + j\hat{s}_{Q,n}^{(i)} \quad (20)$$

For 8 PSK, as proved in Appendix C.1,

$$\hat{s}_{I,n}^{(i)} = \frac{(1-t_2)(t_0-t_1)-(t_0+t_1)[1+\sqrt{2}+(1-\sqrt{2})t_2]}{4\sqrt{2}} \quad (21)$$

and

$$\hat{s}_{Q,n}^{(i)} = \frac{(t_1-t_0)[1+\sqrt{2}-(1-\sqrt{2})t_2]-(1+t_2)(t_0+t_1)}{4\sqrt{2}} \quad (22)$$

where

$$t_r \triangleq \tanh\left(\frac{L_e^{(i)}[x_n^r]}{2}\right) \quad (23)$$

For 16 QAM,

$$\hat{s}_{I,n}^{(i)} \triangleq \sum_{l=0}^{3} a_{I,l} \cdot P_a^{(i+1)}(a_{I,l}) \quad (24)$$

$\hat{s}_{Q,n}^{(i)}$ can be similarly defined. As proved in Appendix C.2,

$$\hat{s}_{I,n}^{(i)} = t_0 \cdot (2-t_1). \quad (25)$$

Similarly, it can be easily shown that

$$\hat{s}_{Q,n}^{(i)} = t_2 \cdot (2-t_3).$$

Note that after the desired number of iterations, final decision for s_n is made based on the *a posteriori* LLR of s_n for both 8 PSK and 16 QAM.

4.3 Post-detection Error Power

The post-detection error power in (3) which is used in the forward-filter at the $(i+1)$th iteration can be written as

$$(\sigma_d^{(i)})^2 = \frac{1}{N}\sum_{n=0}^{N-1}\sum_{l=0}^{M-1}|a_l - \hat{s}_n^{(i)}|^2 P_a^{(i+1)}(a_l). \quad (26)$$

For 8 PSK, (26) can be derived to be

$$(\sigma_d^{(i)})^2 = \frac{1}{N}\sum_{n=0}^{N-1}\left(1-|\hat{s}_n^{(i)}|^2\right) \quad (27)$$

as proved in Appendix D.1.

For 16 QAM, the post-detection error power can be decomposed into its in-phase and quadrature components, that is, $(\sigma_d^{(i)})^2 = (\sigma_{d,I}^{(i)})^2 + (\sigma_{d,Q}^{(i)})^2$. From (26), as proved in Appendix D.2,

$$(\sigma_{d,I}^{(i)})^2 = \frac{1}{N}\sum_{n=0}^{N-1}\left(5-|\hat{s}_{I,n}^{(i)}|^2 - 4t_1\right). \quad (28)$$

where t_1 is in (23). Similarly, it can be shown that

$$(\sigma_{d,Q}^{(i)})^2 = \frac{1}{N}\sum_{n=0}^{N-1}\left(5-|\hat{s}_{Q,n}^{(i)}|^2 - 4t_3\right). \quad (29)$$

V. Simulation Results

In this section, bit error rate (BER) performance of EST-based modulation employing 8 PSK and 16 QAM are provided. As in [1], EST constructed by concatenating random-permutation matrix and normalized Fourier-transform matrix is used with symbol block size $N=2048$. Performances of both hard-decision and soft-decision receivers are

provided for EST-based modulation. Besides, MFB, which is the performance of an ideal receiver that can completely eliminate ISI by the aid of genie, is provided for comparison.

Fig. 2 shows the performance of EST-based modulation employing 8 PSK for the B channel in [12, page. 631], whose impulse response is

$$h_n = 0.407\delta_n + 0.815\delta_{n-1} + 0.407\delta_{n-2}.$$

At a sufficiently high SNR, the performances of both hard-decision and soft-decision receivers are improved as iteration proceeds until they come close to MFB. At BER $=10^{-4}$ and after the tenth iteration, the soft-decision receiver performs 0.53 dB better than the hard-decision receiver and very close to the MFB.

Fig. 3 shows the performance of EST-based modulation for 16 QAM when the same channel used in Fig. 2 is employed. For the hard-decision receiver, severe error propagation occurs below 27dB as iteration proceeds. However, the soft-decision scheme prevents severe error propagation and shows significantly better performance than hard-decision receiver. At BER=10^{-4} and after the third iteration, the soft-decision receiver outperforms the hard-decision receiver by 0.62 dB. After the tenth iteration, the soft-decision receiver outperforms the hard-decision receiver by 3.39 dB, but there is still 8.33 dB gap from the MFB for 16 QAM. For 16 QAM, the proposed scheme is shown to have nonnegligible performance gap from the MFB. This is because the post-detection error power is usually higer for higer-order modulations.

Fig. 4 shows the BER performance of the EST-based modulation after the tenth iteration in a fading channel. For the generation of fading channel, uniform channel power-delay profile with eight symbol-spaced taps has been used. Each tap is considered as independent complex Gaussian random variable with zero mean and variance 1/8. The performance is averaged over 100,000 random channel realizations. The performance of the soft-decision receiver for both 8 PSK and 16 QAM are provided together with MFB. For comparison, performance of EST-based modulation using QPSK and soft-decision receiver in [1] is also provided. For QPSK and 8 PSK, the soft-decision receiver performs very close to the MFB at BER =10^{-4}. However, for 16 QAM, the performance gap between the soft-decision receiver and the MFB at

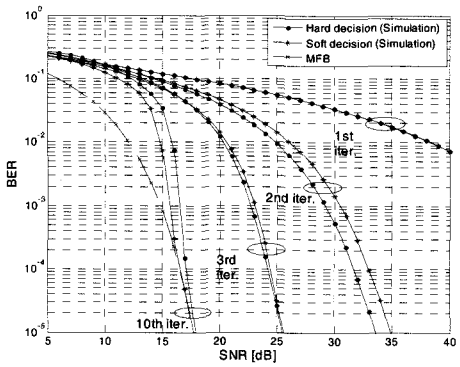

Fig. 2. 8 PSK, Proakis B channel

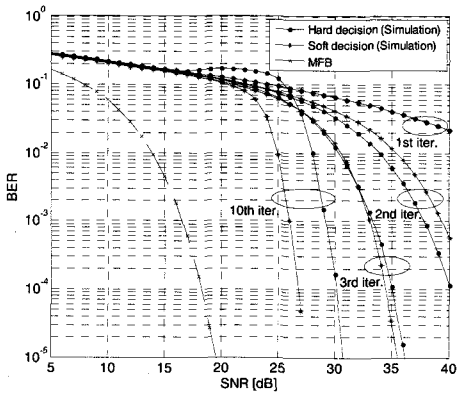

Fig. 3. 16 QAM, Proakis B channel

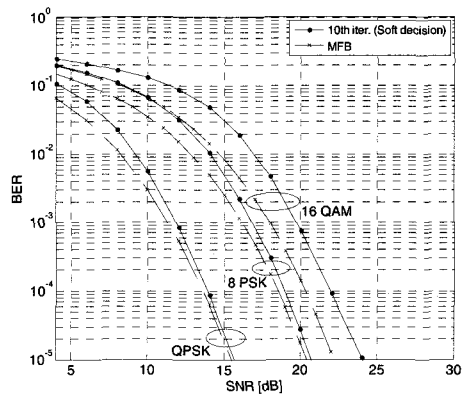

Fig. 4. 16 Fading channel

the BER $=10^{-4}$ is about 1.62 dB.

VI. Conclusion

In this paper, EST-based modulation originally proposed for QPSK has been extended to both 8 PSK and 16 QAM. Optimum receive filters for both hard-decision and soft-decision schemes are derived and simulation results are provided. Simulation results show that EST-based modulation is also an effective technique for high modulations such as 8 PSK and 16 QAM.

Appendix A

Derivation of (6) and (7)

Here, we drop the time index n in s_n and d_n for simplicity. Omitting the time index, (5) becomes

$$\left(\sigma_d^{(i)}\right)^2 = \mathcal{E}\left\{|d^{(i)}|^2 | d^{(i)} \neq 0\right\} \cdot p^{(i)} \tag{30}$$

where $d^{(i)} = s - \hat{s}^{(i)}$. As derived in [13], SER can be written as

$$p^{(i)} \approx \begin{cases} 2Q\left(\sqrt{0.293\gamma^{(i)}}\right) & \text{for 8 PSK} \\ 3Q\left(\sqrt{\frac{1}{5}\gamma^{(i)}}\right) & \text{for 16 QAM} \end{cases}$$

Define $d_{r,l} \triangleq |a_r - a_l|$ to be the Euclidean distance between a_r and a_l in the M-ary alphabet in Table 1, then the conditional expectation in (30) can be represented as

$$\mathcal{E}\left\{|d^{(i)}|^2 | d^{(i)} \neq 0\right\} = \sum_{l=0}^{M-1} c_l \cdot P^{(i)}(s = a_l) \tag{31}$$

where

$$\begin{aligned} c_l &= \sum_{\substack{r=0,\cdots,M-1 \\ r \neq l}} d_{r,l}^2 \cdot P\left(\hat{s} = a_r | s = a_l, \hat{s} \neq s\right) \\ &= \sum_{\substack{r=0,\cdots,M-1 \\ r \neq l}} d_{r,l}^2 \cdot \frac{P\left(\hat{s} = a_r | s = a_l\right)}{P\left(\hat{s} \neq s | s = a_l\right)}. \end{aligned} \tag{32}$$

1. 8 PSK Case

For 8 PSK modulation, due to the symmetry, $c_0 = c_1 = \cdots = c_7$. Therefore, without loss of generality, (31) can be written as

$$\mathcal{E}\left\{|d^{(i)}|^2 | d^{(i)} \neq 0\right\} = c_0 \sum_{l=0}^{M-1} P^{(i)}(s = a_l) = c_0 \tag{33}$$

Then, from (32), (33), and the fact $P\left(\hat{s} \neq s | s = a_0\right) = p^{(i)}$, (30) can be represented as

$$\left(\sigma_d^{(i)}\right)^2 = \sum_{r=1}^{7} (d_{r,0})^2 P\left(\hat{s} = a_r | s = a_0\right), \tag{34}$$

where $d_{r,0}$'s can be easily calculated to be $d_{1,0} = d_{7,0} = 0.765$, $d_{2,0} = d_{6,0} = \sqrt{2}$, $d_{3,0} = d_{5,0} = 1.8477$, $d_{4,0} = 2$, and

$$P\left(\hat{s} = a_r | s = a_0\right) \approx Q\left(\sqrt{\frac{d_{r,0}^2 \gamma^{(i)}}{2}}\right),$$

which is the pairwise-error probability (PEP)[13]. From (34), (6) can be obtained.

2. 16 QAM case

The symbols $\{a_l\}_{l=0}^{15}$ for 16 QAM are shown in Fig. 5. To calculate (31), we need to consider only one of the four quadrants due to the symmetry of 16 QAM constellation. Choosing the third quadrant, (31) can be written as

$$\mathcal{E}\left\{|d^{(i)}|^2 | d^{(i)} \neq 0\right\} = 4 \sum_{l=0,1,4,5} c_l \cdot P^{(i)}(s = a_l),$$

where we assume $P^{(i)}(s = a_l) = 1/16$ for simplicity and we need to calculate c_0, c_1, c_4, c_5. Now, consider calculating c_0. In (32), $d_{r,0}$'s can be easily calculated to be

$d_{1,0} = d_{4,0} = 4, d_{2,0} = d_{8,0} = 16, d_{3,0} = d_{12,0} = 64,$
$d_{5,0} = 2\sqrt{2}$, $d_{6,0} = d_{9,0} = 2\sqrt{5}$, $d_{7,0} = d_{13,0} = 2\sqrt{17}$,
$d_{10,0} = 4\sqrt{2}, d_{11,0} = d_{14,0} = 4\sqrt{5}$, and
$d_{15,0} = 8\sqrt{2}$.

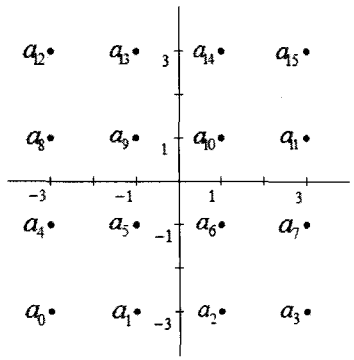

Fig. 5. 16 QAM constellation

The numerator in (32) when $r=1$ can be written as

$$\begin{aligned} &P\left(\hat{s}=a_1 \mid s=a_0\right) \\ &\quad=P\left(-2\le z_{I,n}^{(i)}<0\right)P\left(z_{Q,n}^{(i)}<-2\right) \\ &\quad=\left[Q\left(\sqrt{\frac{1}{5}\gamma^{(i)}}\right)-Q\left(3\sqrt{\frac{1}{5}\gamma^{(i)}}\right)\right] \\ &\quad\times\left[1-Q\left(\sqrt{\frac{1}{5}\gamma^{(i)}}\right)\right] \end{aligned} \tag{35}$$

where $\gamma^{(i)}=10/\left(\sigma_e^{(i)}\right)^2$ for 16 QAM. It can be similarly derived for $r=2,\cdots,15$. The denominator in (32) becomes

$$\begin{aligned} &P\left(\hat{s}\neq s \mid s=a_0\right) \\ &\quad=1-P\left(z_{I,n}^{(i)}<-2\right)P\left(z_{Q,n}^{(i)}<-2\right) \\ &\quad\approx 2Q\left(\sqrt{\frac{1}{5}\gamma^{(i)}}\right) \end{aligned} \tag{36}$$

Then, from the above, c_0 in (32) is

$$c_0\approx\frac{4Q\left(\sqrt{\frac{1}{5}\gamma^{(i)}}\right)+12Q\left(3\sqrt{\frac{1}{5}\gamma^{(i)}}\right)+20Q\left(5\sqrt{\frac{1}{5}\gamma^{(i)}}\right)}{Q\left(\sqrt{\frac{1}{5}\gamma^{(i)}}\right)}.$$

Similarly, it can be easily shown that

$$c_1=c_4\approx\frac{4Q\left(\sqrt{\frac{1}{5}\gamma^{(i)}}\right)+8Q\left(3\sqrt{\frac{1}{5}\gamma^{(i)}}\right)+\frac{20}{3}Q\left(5\sqrt{\frac{1}{5}\gamma^{(i)}}\right)}{Q\left(\sqrt{\frac{1}{5}\gamma^{(i)}}\right)}$$

and

$$c_5\approx\frac{4Q\left(\sqrt{\frac{1}{5}\gamma^{(i)}}\right)+6Q\left(3\sqrt{\frac{1}{5}\gamma^{(i)}}\right)}{Q\left(\sqrt{\frac{1}{5}\gamma^{(i)}}\right)}.$$

From above, (7) can be finally obtained.

Appendix B

Derivation of (15) and (18)

1. 8 PSK

For 8 PSK, the symbols for which $b_l^0=1$ are a_4,a_5,a_6,a_7, while the symbols for which $b_l^0=0$ are a_0,a_1,a_2,a_3. From (10) and (12), the *extrinsic* LLR of x_n^0 can be expressed as

$$\begin{aligned} &L_e^{(i)}\left[x_n^0\right] \\ &\quad\approx\ln\left[\sum_{l=4}^{7}\exp\left(-\frac{\left|z_n^{(i)}-a_l\right|^2}{\left(\sigma_e^{(i)}\right)^2}\right)P_a\left(b_l^1\right)P_a\left(b_l^2\right)\right] \\ &\quad\quad-\ln\left[\sum_{l=0}^{3}\exp\left(-\frac{\left|z_n^{(i)}-a_l\right|^2}{\left(\sigma_e^{(i)}\right)^2}\right)P_a\left(b_l^1\right)P_a\left(b_l^2\right)\right] \\ &\quad=\ln\left[\sum_{l=4}^{7}\exp\left(g_l^{(i)}\right)\right]-\ln\left[\sum_{l=0}^{3}\exp\left(g_l^{(i)}\right)\right] \end{aligned} \tag{37}$$

where

$$g_l^{(i)}\triangleq-\frac{\left|z_n^{(i)}-a_l\right|^2}{\left(\sigma_e^{(i)}\right)^2}+\sum_{m:\,b_l^m=1}L_a^{(i)}\left[x_n^m\right]. \tag{38}$$

Note that $m:b_l^m=1$ in (38) denotes the bit indices such that $b_l^m=1$ corresponding to the given a_l.

Using (14) and (38), the first term in (37) can be written as

$$\ln\left[\sum_{l=4}^{7}\exp\left(g_l^{(i)}\right)\right]=\widehat{\max}\left(g_4^{(i)},g_5^{(i)},g_6^{(i)},g_7^{(i)}\right).$$

The second term in (37) can be similarly derived. Then, (37) can be written as

$$L_e^{(i)}\left[x_n^0\right]=\widehat{\max}\left(g_4^{(i)},\ g_5^{(i)},\ g_6^{(i)},\ g_7^{(i)}\right)-\widehat{\max}\left(g_0^{(i)},\ g_1^{(i)},\ g_2^{(i)},\ g_3^{(i)}\right). \tag{39}$$

Finally, (15) can be obtained after calculating all $g_l^{(i)}$'s in (38) and using (39).

2. 16 QAM

For 16 QAM, from (10) the *extrinsic* LLR of x_n^0 can be written as

$$\begin{aligned}L_e^{(i)}\left[x_n^0\right]&\approx\ln\left[\sum_{l=2}^{3}\exp\left(-\frac{\left|z_{I,n}^{(i)}-a_{I,l}\right|^2}{\left(\sigma_{e,I}^{(i)}\right)^2}\right)P_a\left(b_l^1\right)\right]\\&\quad-\ln\left[\sum_{l=0}^{1}\exp\left(-\frac{\left|z_{I,n}^{(i)}-a_{I,l}\right|^2}{\left(\sigma_{e,I}^{(i)}\right)^2}\right)P_a\left(b_l^1\right)\right]\\&=\ln\left[\sum_{l=2}^{3}\exp\left(g_{I,l}^{(i)}\right)\right]-\ln\left[\sum_{l=0}^{1}\exp\left(g_{I,l}^{(i)}\right)\right]\\&=\widehat{\max}\left(g_{I,2}^{(i)},\ g_{I,3}^{(i)}\right)-\widehat{\max}\left(g_{I,0}^{(i)},\ g_{I,1}^{(i)}\right)\end{aligned} \tag{40}$$

where

$$g_{i,l}^{(i)}\triangleq\begin{cases}-\dfrac{\left|z_{I,n}^{(i)}-a_{I,l}\right|^2}{\left(\sigma_{e,I}^{(i)}\right)^2}+L_a^{(i)}\left[x_n^1\right], & \left(b_l^1=1\right)\\ -\dfrac{\left|z_{I,n}^{(i)}-a_{I,l}\right|^2}{\left(\sigma_{e,I}^{(i)}\right)^2}, & \left(b_l^1=0\right)\end{cases}$$

Finally, (18) can be obtained after calculating all $g_{I,l}^{(i)}$'s and using (40).

Appendix C

Derivation of (21), (22) and (25)

The symbol *a priori* probability in (20) can be written as

$$P_a^{(i+1)}(a_l)=\prod_{r=0}^{M-1}P_a^{(i+1)}(b_l^r). \tag{41}$$

From

$$P_a^{(i+1)}(x_n^r=1)=1-P_a^{(i+1)}\left(x_n^r=0\right) \tag{42}$$

and (8), it can be shown that

$$\begin{aligned}P_a^{(i+1)}(x_n^r=0)&=\frac{1}{1+\exp\left(L_a^{(i+1)}\left[x_n^r\right]\right)}\\&=\frac{1}{2}-\frac{1}{2}\tanh\left(\frac{L_a^{(i+1)}\left[x_n^r\right]}{2}\right)\end{aligned} \tag{43}$$

Also, from (42) and (43),

$$P_a^{(i+1)}(x_n^r=1)=\frac{1}{2}+\frac{1}{2}\tanh\left(\frac{L_a^{(i+1)}\left[x_n^r\right]}{2}\right). \tag{44}$$

1. 8 PSK

For 8 PSK, from (20) and (41), the soft decision can be represented in terms of the bit *a posteriori* probabilities as

$$\hat{s}_n^{(i)}=\sum_{l=0}^{7}a_l P_a^{(i+1)}\left(b_l^0\right)P_a^{(i+1)}\left(b_l^1\right)P_a^{(i+1)}\left(b_l^2\right). \tag{45}$$

Finally, (21) and (22) can be derived from (43), (44), and (45), where

$$t_r=\tanh\left(\frac{L_a^{(i+1)}\left[x_n^r\right]}{2}\right)=\tanh\left(\frac{L_e^{(i)}\left[x_n^r\right]}{2}\right) \tag{46}$$

in (23). Note that in (46), we used (9).

2. 16 QAM

For 16 QAM, using the in-phase version of (41), (24) can be represented as

$$\hat{s}_{I,n}^{(i)}=\sum_{l=0}^{3}\left[a_{I,l}P_a^{(i+1)}(b_l^0)P_a^{(i+1)}(b_l^1)\right]. \tag{47}$$

Finally, (25) can be derived from (43), (44), and (47).

Appendix D

Derivation of (27) and (28)

1. 8 PSK

For 8 PSK, using $|a_l|=1$ for all l, $\sum_{l=0}^{7}P_a^{(i+1)}(a_l)=1$, and (20), the inner summation in (26) can be written as

$$\sum_{l=0}^{M-1}\left|a_l-\hat{s}_n^{(i)}\right|^2 P_a^{(i+1)}(a_l)=1-\left|\hat{s}_n^{(i)}\right|^2 \quad . \qquad (48)$$

Finally, (27) can be derived from (26) and (48).

2. 16 QAM

For 16 QAM, the in-phase power of (26) is

$$\left(\sigma_{d,I}^{(i)}\right)^2=\frac{1}{N}\sum_{n=0}^{N-1}\sum_{l=0}^{3}\left|a_{I,l}-\hat{s}_{I,n}^{(i)}\right|^2 P_a^{(i+1)}(a_{I,l}) \quad . \qquad (49)$$

The inner summation term in (49) can be written as

$$\sum_{l=0}^{3}(a_{I,l}-\hat{s}_{I,n}^{(i)})^2 P_a^{(i+1)}(a_{I,l})=u_1+u_2+u_3, \qquad (50)$$

where

$$u_1=-2\hat{s}_{I,n}^{(i)}\underbrace{\sum_{l=0}^{3}a_{I,l}P_a^{(i+1)}(a_{I,l})}_{=\hat{s}_{I,n}^{(i)}}=-2\left(\hat{s}_{I,n}^{(i-1)}\right)^2,$$

$$u_2=\left(\hat{s}_{I,n}^{(i)}\right)^2\underbrace{\sum_{l=0}^{3}P_a^{(i+1)}(a_{I,l})}_{=1}=\left(\hat{s}_{I,n}^{(i)}\right)^2,$$

and

$$u_3=\sum_{l=0}^{3}(a_{I,l})^2 P_a^{(i)}(a_{I,l}).$$

Using

$$P_a^{(i)}(a_{I,l})=P_a^{(i)}\left(x_n^0=b_l^0\right)\cdot P_a^{(i)}\left(x_n^1=b_l^1\right),$$
$$P_a^{(i)}\left(x_n^r=1\right)+P_a^{(i)}\left(x_n^r=0\right)=1,$$

and (43), it can be easily shown that

$$u_3=5-4t_1. \qquad (51)$$

Finally, from (49) and (50), (28) can be obtained.

References

[1] T. Hwang and Y. (G.) Li, "Optimum filtering for energy-spreading transform-based equalization," *IEEE Trans. Signal Process.*, vol.55, no.3, pp.1182-1187, Mar. 2007.

[2] S. Weinstein and P. Ebert, "Data transmission by frequency-division multiplexing using the discrete Fourier transform," *IEEE Trans. Commun. Technol.*, vol. COM-19, no.5, pp.628-634, Oct. 1971.

[3] L. J. Cimini, Jr., "Analysis and simulation of a digital mobile channel using orthogonal frequency division multiplexing," *IEEE Trans. Commun.*, vol. COM-33, no. 7, pp. 665-675, Jul. 1985.

[4] Y. (G.) Li and G. Stuber, *Orthogonal Frequency Division Multiplexing for Wireless Communications*, Boston, MA: Springer, 2006.

[5] T. Hwang, C. Yang, G. Wu, S. Li, and Y. (G.) Li, "OFDM and Its Wireless Applications: A Survey," *IEEE Trans. Veh. Technol.*, vol.~58, no.~4, PP.~1673-1694 , May 2009.

[6] D. Falconer, S. L. Ariyavisitakul, A. Benyamin-Seeyar, and B. Eidson, "Frequency-domain equalization for single-carrier broadband wireless systems," *IEEE Commun. Mag.*, vol. 40, no. 4, pp. 58-66, Apr. 2002.

[7] A. J. Goldsmith and S. Chua, "Variable-Rate Variable-Power MQAM for Fading Channels," *IEEE Trans. Commun.*, vol. 45, no. 10, pp. 1218-1230, Oct. 1997.

[8] S. T. Chung and A. J. Goldsmith, "Degrees of Freedom in Adaptive Modulation: A Unified View," *IEEE Trans. Commun.*, vol. 49, no. 9, pp. 1561-1571, Sep. 2001.

[9] H. K. Mohammed, R. Tripathi, and K. Kant, "Performance of Adaptive Modulation in Multipath Fading Channel," *in Proc. ICACT*, Feb. 2006, vol. 2, pp. 1277 - 1282.

[10] P. Magniez, B. Muquet, P. Duhamel, and M. de Courville, "Improved turbo-equalization with application to bit interleaved modulations," *in Proc. Asilomar Conf. on Signals, Syst. Comput., Pacific Grove, CA*, Oct. 2000, vol. 2, pp. 1786 - 1790.

[11] A. Dejonghe and L. Vandendorpe, "Turbo-equalisation for multilevel modulation:

an efficient low-complexity scheme,'' *in Proc. IEEE Int. Conf. Commun.*, New York, USA, Apr. 28-May 2, 2002, vol.~3, pp.~1863-1867.
〔12〕 J. G. Proakis, *Digital Communications*, 4th ed., New York: McGraw-Hill, 2001
〔13〕 J. R. Barry, *Digital Communications*, 3rd ed. New York: Springer 2004.

권 병 욱 (Byung-uk Kwon) 준회원

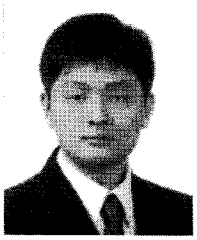

2009년 2월 건국대학교 전자공학과 졸업
2009년 3월 연세대학교 전기전자공학부 석사
<관심분야> 전자공학, 통신공학, OFDM, MIMO

황 태 원 (Teawon Hwang) 종신회원

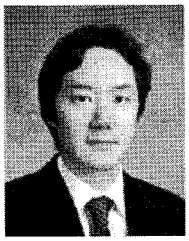

1993년 2월 연세대학교 전자공학과 졸업
1993년 3월~1995년 2월 Georgia Institute of Technology 전기 컴퓨터 공학 석사 졸업
1995년 3월~2000년 ETRI 연구원
2001년 3월~2005년 2월 Georgia Institute of Technology 전기 컴퓨터 공학 박사 졸업
2005년~2005년 Qualcom 인턴
2005년~2006년 YGL Telecom 연구원
2006년~현재 연세대학교 전기전자공학부 교수
<관심분야> 전자공학, 통신공학, OFDM, MIMO